Journal of Molecular Structure 995 (2011) 9–19

Contents lists available at ScienceDirect

Journal of Molecular Structure

journal homepage: www.elsevier.com/locate/molstruc

Solid and solution structures of bulky *tert*-butyl substituted salicylaldimines

Jahir Uddin Ahmad, Martin Nieger, Markku R. Sundberg, Markku Leskelä, Timo Repo *

Department of Chemistry, Laboratory of Inorganic Chemistry, University of Helsinki, P.O. Box 55, FI-00014 Helsinki, Finland

ARTICLE INFO

Article history:
Received 24 September 2010
Received in revised form 11 January 2011
Accepted 14 February 2011
Available online 1 March 2011

Keywords:
Schiff bases
Salicylaldimine
Hydrogen bond
Crystal structure
Tautomerization

ABSTRACT

A series of *tert*-butyl substituted salicylaldimines was synthesized and characterized by IR, ^{1}H NMR, ^{13}C NMR, UV–vis, X-ray diffraction and elemental analyses to investigate the effect of two bulky *tert*-butyl groups on the keto-enol tautomerization in solution and solid state. According to X-ray studies all salicylaldimines have an enol tautomeric form in solid state and due to strong O–H···N hydrogen bonding they form a nearly planar intramolecular six-membered ring. Based on NMR, IR and UV–vis studies, the enol form is also present in solutions. Computational studies carried out by the density function theory (DFT) method verifies that in each sterically hindered keto-enol pair the enol form is more stable, although the differences in energy vary from 5.5 to 10.1 kJ/mol (in terms of total energy obtained from Gaussian for the optimized moieties). For the *tert*-butyl substituted salicylaldimines, solvatochromism is not observed in polar hydrogen bonding solvents. As *N*-alkyl and *N*-alkylphenyl substituted salicylaldimines without *tert*-butyl groups have a solvatochromic band, the sterically bulky *tert*-butyl groups seem to have a key role in stabilizing the intramolecular hydrogen bonding.

1. Introduction

Schiff base ligands are universal in inorganic chemistry due to their straightforward preparation, high yield and easy purification. Their strong coordination affinities for metal ions are of great interest in the synthesis of transition metal complexes, which play an important role in many fields of chemistry and biochemistry [1,2]. For example, Schiff base complexes have been used as highly efficient catalysts for cyclopropanation [3–6], enantioselective ring opening of mesoaziridine [7], oxidation [8–11], polymerization [12–16], epoxidation [17–19] and Hetero Diels–Alder reactions [20]. In biochemistry, Schiff base copper complexes are known to exhibit good antibacterial activity [21] and have considerable antimalarial activity [22]. It is worth noting that Schiff base ligands alone, such as *N*-hydroxy-*N*^{1}-aminoguanidines, have antitumor and antiviral activities and can also act as inhibitors of leukemia cell growth [23].

Salicylaldimines are particularly interesting as such because of their self-isomerization or tautomerism properties, which are associated with changes in the π-electron density distribution within the molecule and which subsequently cause changes in molecular conformations [24]. In solid state, molecular conformations can be influenced by crystal packing forces, giving different photochromic and thermochromic properties to crystals of the same salicylaldimine. The photochromic behavior arises from the shift in equilibrium between enol and *trans*-keto forms, and thermochromism arises from the shift in equilibrium between enol and *cis*-keto isomers [25,26]. In photochromic materials, salicylaldimines are non-planar (i.e. they lack O–H···N hydrogen bonding), while in thermochromic materials they are planar [27]. As a result, molecules in photochromic materials are packed rather loosely in a crystal and may undergo some conformational changes, while thermochromic materials are packed tightly to form one-dimensional columns [28].

The position and nature of substituents in the phenyl ring of salicylaldimines influence the keto-enol tautomerization [29] and they can also cause a dramatic change in the catalytic properties of salicylaldimine complexes [30]. Salicylaldimines with *tert*-butyl groups in the phenyl moiety at positions 3 and 5 are particularly interesting as they enable peripherally-bound, stable phenoxyl radical complexes to form [31]. For example, copper complexes based on 3,5-di-*tert*-butyl salicylaldimines form highly efficient catalytic systems for the aerobic oxidation of primary benzylic, allylic and heterocyclic alcohols under mild reaction conditions [30].

In solid state, the keto tautomer (O···H–N) is particularly stabilized by functional groups which facilitate the formation of intermolecular H-bonds [32]. On the other hand, the enol form (O–H···N) appears to be predominant in solution when bulky substituents on the salicyl moiety are present [33]. We report herein a detailed study of 3,5-di-*tert*-butyl salicylaldimines that was done to gain further insight into their structure in solution and in solid state. The series consists of seven *tert*-butyl substituted salicylaldimines, including some with electron releasing (Me) or withdrawing

* Corresponding author. Tel.: +358 9191 50194; fax: +358 9191 50198.
E-mail address: timo.repo@helsinki.fi (T. Repo).

0022-2860/$ - see front matter © 2011 Elsevier B.V. All rights reserved.
doi:10.1016/j.molstruc.2011.02.033

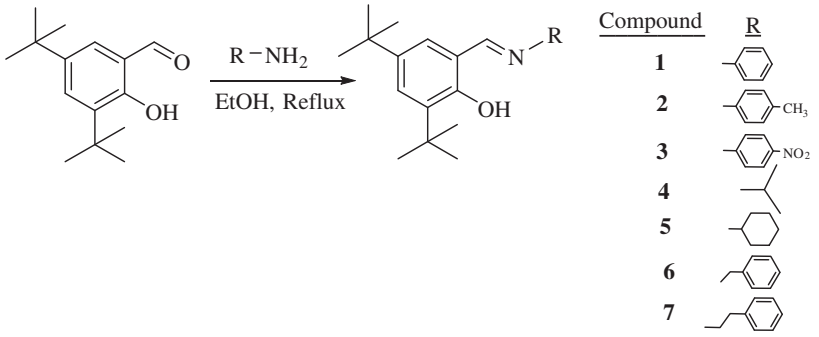

Scheme 1.

(NO_2) groups, the main focus being on the structures in solution and solid state (Scheme 1).

2. Experimental

2.1. General techniques

All chemicals were obtained from commercial sources and were used without further purification. Melting points were obtained with an electrothermal melting point apparatus and are not corrected. ^{1}H and ^{13}C NMR spectra were collected on a Varian Mercury 300 MHz spectrometer. Chemical shifts for ^{1}H NMR and ^{13}C NMR were referenced with respect to $CHCl_3$ and TMS, respectively. IR spectra were collected on a Perkin Elmer Spectrum GX spectrometer and a Perkin Elmer Spectrum one spectrometer for solution and solid samples, respectively. UV–vis spectra were recorded with a Hewlett Packard 8453 spectrophotometer from EtOH, $CHCl_3$, toluene and n-hexane solutions. Elemental analyses were made using an EA 1110 CHNS–OCE instrument. EI–mass spectra were run with a JOEL JMS–SX 102 mass spectrometer (ionization voltage 70 eV) from solid samples.

2.2. X-ray crystallography

Dilute methanol solutions of **1** and **4**–**6** were kept at room temperature and by slow evaporation of solvent, single crystals suitable for X-ray studies were obtained. Crystals of **2** and **7** were obtained from saturated toluene and n-heptane solutions, respectively. Compound **2** crystallizes with two and **4** with three independent molecules in the asymmetric unit.

Crystal data, data collection parameters and details of the refinements are summarized in Table 1. All single-crystal X-ray diffraction studies were carried out on a Bruker–Nonius Kappa-CCD diffractometer at 123(2) K and 173(2) K, using Mo Kα radiation (λ = 0.71073 Å). Direct methods (SHELXS-97) were used for structure solution and refinement was carried out using SHELXL-97 (full-matrix least-squares on F^2) [34]. Hydrogen atoms were localized by difference electron density determination and refined using a riding model, and H(O) atoms were refined free. In **2** and **6** a *tert*-butyl group at carbon 4 is disordered. The absolute structure of **1** and **5** could not be determined reliably by refinement of Flack's *x*-parameter [35].

Crystallographic data (excluding structure factors) for the structures reported in this work have been deposited with the Cambridge Crystallographic Data Centre as Supplementary Publication Nos. CCDC 734930 (**1**), CCDC 734931 (**2**), CCDC 734932 (**3**), CCDC 734933 (**4**), CCDC 734934 (**5**), CCDC 734935 (**6**) and CCDC 734936 (**7**). Copies of the data can be obtained free of charge on application to The Director, CCDC, 12 Union Road, Cambridge DB2 1EZ, UK (Fax: int. code + (1223)336 033; e-mail: deposit@ccdc.cam.ac.uk).

2.3. Ligand synthesis

Schiff base ligands **1**–**7** were prepared with high yields (80–90%) as yellow to orange crystalline solids by published procedures [36,37] involving the condensation of 3,5-di-*tert*-butyl-salicylaldehyde with the appropriate amine in refluxing ethanol in the presence of a catalytic amount of formic acid (2–3 drops) as shown in Scheme 1 (for more details concerning the ligand synthesis, see Supplementary materials).

2.4. Computational study

Salicylaldimines **1**–**7** were fully optimized at the B3LYP/6–311G* level of theory. The experimental atomic coordinates obtained from the single-crystal X-ray diffraction studies were used as inputs. The computed IR spectra for the optimized ligands did not show any imaginary frequencies. The results were obtained using the Gaussian03 program suite [38]. NBO analysis was carried out by subroutines of Gaussian03 [39].

3. Results and discussion

3.1. IR and NMR spectra

The IR spectra for **1**–**7** were measured from solid samples and solutions and their corresponding characteristic data are listed in Table 2. For comparison also calculated frequencies for enol and keto forms are included. The calculations were made at B3LYP/6–311G* level of theory and the obtained frequencies are multiplied by scaling factor (0.9632) to compensate the shortcomings due to the electron correlation approximate treatment, anharmonicity effects, basic set deficiencies etc. [40]. For **1** the calculated IR spectra including both enol and keto form together with experimental spectra in solid state and in $CHCl_3$ solution are given in Fig. 1. Accordingly, the calculated and observed IR frequencies confirm the presence of **1** in enol form rather than keto form both in solution and solid state.

In solid state IR spectra, a sharp and intense band is observed in the range 2949–2966 cm^{-1} due to ν(O–H). The presence of this band at such a relatively low frequency is characteristic of these compounds and is an indication of strong hydrogen bonding [41]. In the calculated IR spectra, the most intense stretching vibration is assigned to O–H mode at 2997–3074 cm^{-1}. Very sharp and strong bands in the region of 1433–1440 cm^{-1} are due to stretching of the phenolic C–O band [40(a),42], suggesting that all compounds in the solid state exist as an enol-imino (O–H···N) tautomer. The calculated value for C–O band is in the range 1428–1439 cm^{-1}. The characteristic ν(C=N) band in the solid state is observed in the region 1570–1619 cm^{-1} for **1**–**3**, which have an *N*-phenyl substituent. The *N*-alkyl substituted **4**–**5** give the ν(C=N)

Table 1
Crystal data and structure refinement parameters for **1**–**7**.

	1	**2**	**3**	**4**	**5**	**6**	**7**
Empirical formula	$C_{21}H_{27}NO$	$C_{22}H_{29}NO$	$C_{22}H_{29}N_2O_3$	$C_{18}H_{29}NO$	$C_{21}H_{33}NO$	$C_{22}H_{29}NO$	$C_{23}H_{31}NO$
Formula weight	309.44	323.46	354.44	275.42	315.48	323.46	337.49
Temperature (K)	123(2)	123(2) K	173(2)	123(2)	173(2)	123(2)	173(2)
Radiation, wavelength	Mo Kα, 0.71073 Å	Mo Kα, 0.71073 Å	Mo Kα, 0.71073 Å	Mo Kα, 0.71073 Å	Mo Kα, 0.71073 Å	Mo Kα, 0.71073 Å	Mo Kα, 0.71073 Å
Crystal system	Orthorhombic	Monoclinic	Orthorhombic	Triclinic	Orthorhombic	Monoclinic	Monoclinic
Space group	$Pna2_1$ (No. 33)	$P2_1/c$ (No. 14)	Pccn (No. 56)	P-1 (No. 2)	$Pna2_1$ (No. 33)	$P2_1/c$ (No. 14)	$P2_1/c$ (No. 14)
a (Å)	12.305(1)	19.782(2)	13.406(2)	12.020(2)	11.964(8)	17.074(5)	10.418(2)
b(Å)	8.917(1)	10.715(1)	24.064(4)	15.566(2)	9.947(4)	9.889(2)	10.0118(18)
c(Å)	16.568(2)	20.713(2)	12.006(1)	15.920(2)	16.848(4)	11.483(2)	20.286(3)
α (°)	90	90	90	72.11(1)	90	90	90
β (°)	90	117.80(1)	90	80.74(1)	90	93.13(2)	101.035(15)
γ (°)	90	90	90	75.29(1)	90	90	90
V (Å^3)	1817.9(3)	3883.7(7)	3873.2(9)	2730.6(7)	2005.0(16)	1936.0(8)	2076.8(7)
Z	4	8	8	6	4	4	4
D_{cal} (g cm^{-3})	1.131	1.106	1.216	1.005	1.045	1.110	1.079
Absorption coefficient (mm^{-1})	0.068	0.067	0.081	0.061	0.063	0.067	0.065
F(0 0 0)	672	1408	1520	912	696	704	736
Crystal size (mm)	0.50 × 0.45 × 0.40	0.35 × 0.15 × 0.05	0.55 × 0.45 × 0.15	0.45 × 0.30 × 0.20	0.50 × 0.12 × 0.08	0.50 × 0.35 × 0.15	0.50 × 0.40 × 0.20
2 Theta$_{max.}$ (°)	55	55	50	50	50	50	50
Limiting indices	$-15 \le h \le 15$ $-11 \le k \le 11$ $-20 \le l \le 21$	$-20 \le h \le 25$ $-13 \le k \le 13$ $-26 \le l \le 24$	$-15 \le h \le 9$ $-27 \le k \le 28$ $-14 \le l \le 11$	$-14 \le h \le 14$ $-18 \le k \le 18$ $-18 \le l \le 18$	$-14 \le h \le 14$ $-11 \le k \le 11$ $-19 \le l \le 20$	$-20 \le h \le 20$ $-11 \le k \le 9$ $-13 \le l \le 9$	$-12 \le h \le 12$ $-11 \le k \le 10$ $-23 \le l \le 24$
No. of data collected	22,817	31,777	10,132	33,617	20,744	7607	12,641
No. of unique data	4047	8881	3324	9374	3502	3277	3632
$R_{int.}$	0.0296	0.0606	0.0390	0.0468	0.1042	0.0311	0.0558
No. of parameters/ restraints	211/2	436/98	238/1	550/9	211/2	211/80	229/1
R[a] [for $I > 2\sigma(I)$]	0.0330	0.0784	0.0418	0.0525	0.0666	0.0694	0.0475
wR_2[b] (for all data)	0.0795	0.2096	0.0976	0.1247	0.1757	0.1748	0.1161
Goodness of fit	1.07	1.03	1.06	1.06	1.05	1.05	1.05
Absolute structure parameter x	−0.1(11)				−1(3)		
Largest diff. peak and hole (e A^{-3})	0.215/−0.177	0.793/−0.550	0.193/−0.176	0.455/−0.237	0.354/−0.247	0.817/−0.519	0.165/−0.231

[a] $R = \Sigma||F_o| - |F_c||/\Sigma|F_o|$.
[b] $wR_2 = [\Sigma[w(F_o^2 - F_c^2)^2]/\Sigma[w(F_o^2)^2]]^{1/2}$.

band at 1629 cm^{-1} while the band appears at 1631–1635 cm^{-1} for the *N*-alkylphenyl substituted **6** and **7**. The relatively low C═N stretching frequencies in *N*-phenyl salicylaldimines (**1**–**3**) compared to *N*-alkyl (**4**–**5**) or alkylphenyl salicylaldimines (**6**–**7**) are presumably due to the conjugation between the azomethine (CH═N) and the π system of the *N*-phenyl ring. A similar phenomenon is observed in solution [42] as well as in gas phase measurements. The calculated values for ν(C═N) in the enol form are between 1560 and 1636 cm^{-1}. It is noteworthy that in the calculated IR spectra for the keto form, the most intense fundamental vibration frequency is assigned to C═N at 1276–1633 cm^{-1}. The presence of phenolic νC–O at 1433–1440 cm^{-1} and the absence of a band at 1728–1731 cm^{-1} for C═O [37,43] in the $CHCl_3$, toluene and n-hexane spectra of the compounds is the evidence for the predominant species of enol form (N···H–O) with intramolecular hydrogen bonding in the solutions. In keto form, the calculated frequency for C═O is assigned at 1525–1551 cm^{-1} which is eventually absence in the experimental IR spectra of the compounds (**1**–**7**). A narrow band is observed for the compounds in the range 2854–2973 cm^{-1} due to the ν(C–H) stretching mode of the *t*-Bu groups [44].

The presence of the enol form with intramolecular hydrogen bonding in solution can also be ascertained by ^{1}H NMR spectroscopy as well [36,45,46]. The azomethine proton (C**H**═N) resonance is observed within the range of 8.63–8.66 ppm for *N*-phenyl salicylaldimines (**1**–**3**), around 8.36 ppm for *N*-alkyl (**4**–**5**) and 8.27–8.44 for *N*-alkylphenyl (**4**–**7**) salicylaldimines as the electron withdrawing phenyl group de-shields the azomethine proton and shifts the resonance to relatively low field (see Table 2). The C**H**═N resonance appears as a broad singlet for all compounds in $CDCl_3$, providing further evidence that in solution these compounds exist mainly in the enol-imino tautomeric form. In all cases a singlet for O**H** has a distinct down-field resonance in the range of 13.10–14.03 ppm, characteristic for the acidic proton involved in a strong intramolecular hydrogen bond [47]. This phenomenon is further confirmed by ^{13}C NMR spectra (see Table 2) where the phenolic carbon **C**1 resonance exists from 158.3 to 158.8 ppm, whereas it appears further down field in the case of keto-imino tautomers, $(\mathbf{C}1)_{OH}$ = 149–161 ppm and $(\mathbf{C}1)_{NH}$ = 179–183 ppm [47(b),48].

3.2. UV–vis spectra

Electronic spectra of **1**–**7** were recorded in the 200–900 nm range in polar and nonpolar solvents such as $CHCl_3$, EtOH, toluene and n-hexane (Fig. 2). The corresponding data for the salicylaldimines in the different solvents are also listed in Table 3. Previous work on Schiff base derivatives has suggested that enolic intramolecular hydrogen bonding predominates in the ground state in nonpolar environments [49–51]. The absorption band at 400–500 nm can be attributed to the keto form whilst the enol form has no appreciable absorbance in this region [52].

The UV–vis spectra of **4**–**5** and **6**–**7**, having *N*-alkyl and *N*-alkylphenyl groups respectively, in polar and nonpolar solvents show an intense absorption band in the range of 328–333 nm. In general,

Table 2
Characteristic IR (calculated and experimental), ^{1}H and ^{13}C NMR (Experimental) data for **1**–**7**.

Ligand	υ(C–H of t-Bu)	υ(O–H)	υ(C=N)	υ(C=O)	υ(O–$C_{phenolic}$)	^{1}H NMR[c]		^{13}C NMR[c]	
						O**H**	C**H**=N	**C**–OH	**C**H=N
$\mathbf{1}_{enol}$	2994	3017	1614	–	1429	8.64	13.69	164.0	158.5
$\mathbf{1}_{keto}$	2980	–	1629	1538	–				
$\mathbf{1}^{a}_{exp}$	2945/2908/2913/2908	2963/2964/2962/2940	1615/1618/1605/1620	–	1437/1440/1448/1450				
$\mathbf{2}_{enol}$	2992	3678	1627	–	1439	8.63	13.80	163.1	158.4
$\mathbf{2}_{keto}$	2979	–	1629	1531	–				
$\mathbf{2}^{a}_{exp}$	2910/2910/2854/2892	2955/2960/2961/2941	1619/1620/1620/1621		1439/1440/1440/1438				
$\mathbf{3}_{enol}$	2995	3074	1560	–	1427	8.66	13.10	166.6	158.8
$\mathbf{3}_{keto}$	2983	–	1276	1551	–				
$\mathbf{3}^{a}_{exp}$	2947/2940/2854/2972	2966/2964/2962/2988	1570/1577/1579/1581		1433/1433/1437/1434				
$\mathbf{4}_{enol}$	2991	2997	1635	–	1433	8.36	13.97	163.3	158.4
$\mathbf{4}_{keto}$	2979	–	1628	1530	–				
$\mathbf{4}^{a}_{exp}$	2961/2908/2869/2973	2964/2966/2965/2988	1629/1631/1630/1633	–	1441/1441/1441/1436				
$\mathbf{5}_{enol}$	2979	3055	1630	–	1428	8.37	14.03	163.5	158.5
$\mathbf{5}_{keto}$	2978	–	1628	1527	–				
$\mathbf{5}^{a}_{exp}$	2941/2858/2856/2857	2956/2933/2932/2935	1629/1630/1629/1631		1441/1441/1437/1442				
$\mathbf{6}_{enol}$	2992	3023	1636	–	1434	8.44	13.72	166.9	158.3
$\mathbf{6}_{keto}$	2979	–	1633	1525	–				
$\mathbf{6}^{a}_{exp}$	2909/2910/2855/2933	2960/2963/2962/2982	1631/1632/1632/1634	–	1436/1441/1442/1435				
$\mathbf{7}_{enol}$	2993	3000	1636	–	1433	8.27	13.81	166.3	158.4
$\mathbf{7}_{keto}$	2975	–	1633	1532	–				
$\mathbf{7}^{a}_{exp}$	2907/2855/2854/2946	2949/2963/2962/2978	1635/1632/1632/1634	–	1440/1442/1437/1442				
$\mathbf{R}_{enol}$	2979	3041	1642	–	1430	8.64	13.69	164.0	158.5
$\mathbf{R}_{keto}$	2979	–	1642	1532					
$\mathbf{R}^{b}_{exp}$			1648	1731					

[a] Experimental IR (cm^{-1}) in solid state, $CHCl_3$, toluene and n-hexane.
[b] Experimental IR (cm^{-1}) of *N*-methyl-3,5-di-*tert*-butylsalicylaldimine [43].
[c] Experimental ^{1}H and ^{13}C NMR (ppm) in $CDCl_3$.

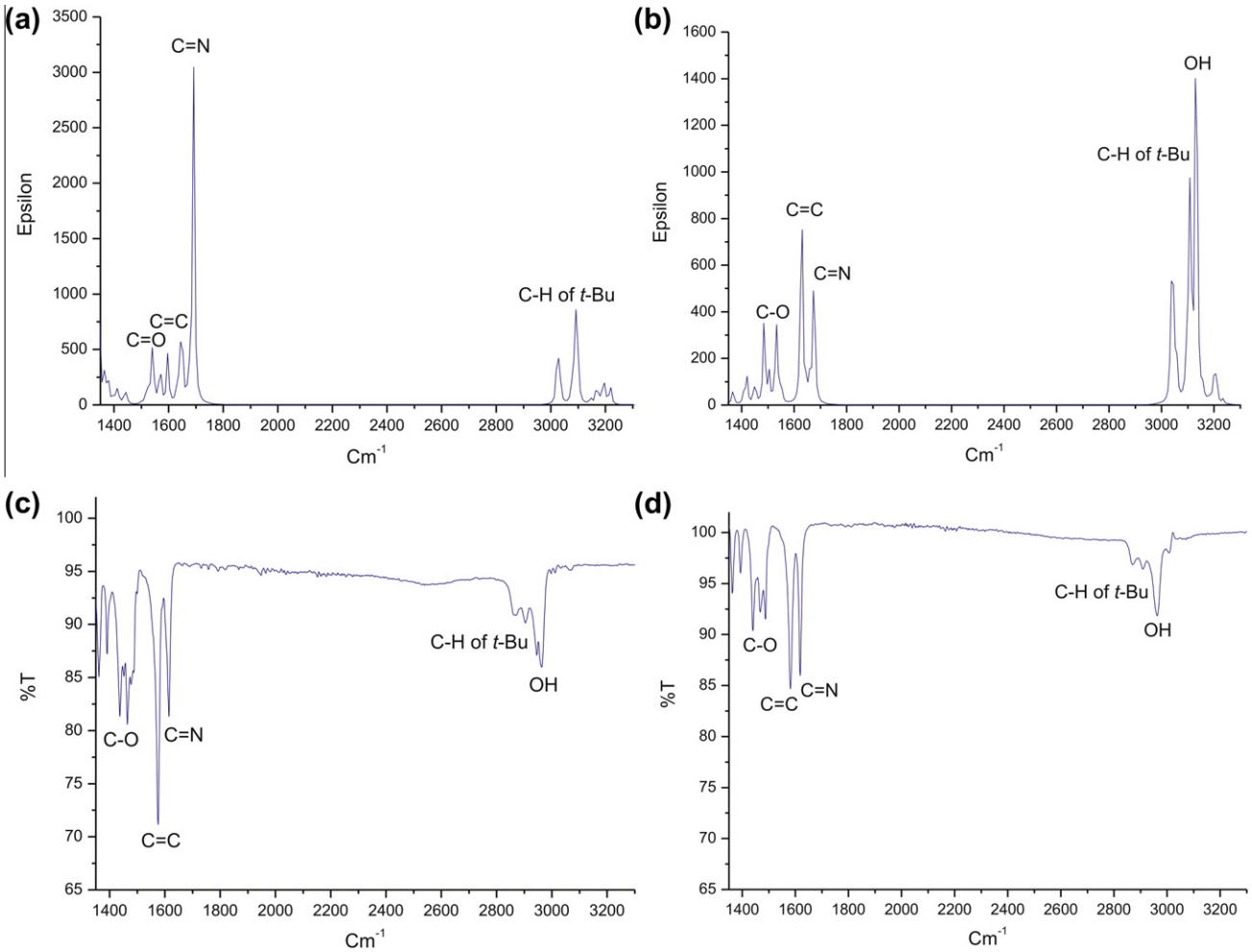

Fig. 1. Calculated (a and b) and experimental (c and d) IR spectra of **1** (a) keto form, (b) enol form, (c) solid state, (d) in $CHCl_3$.

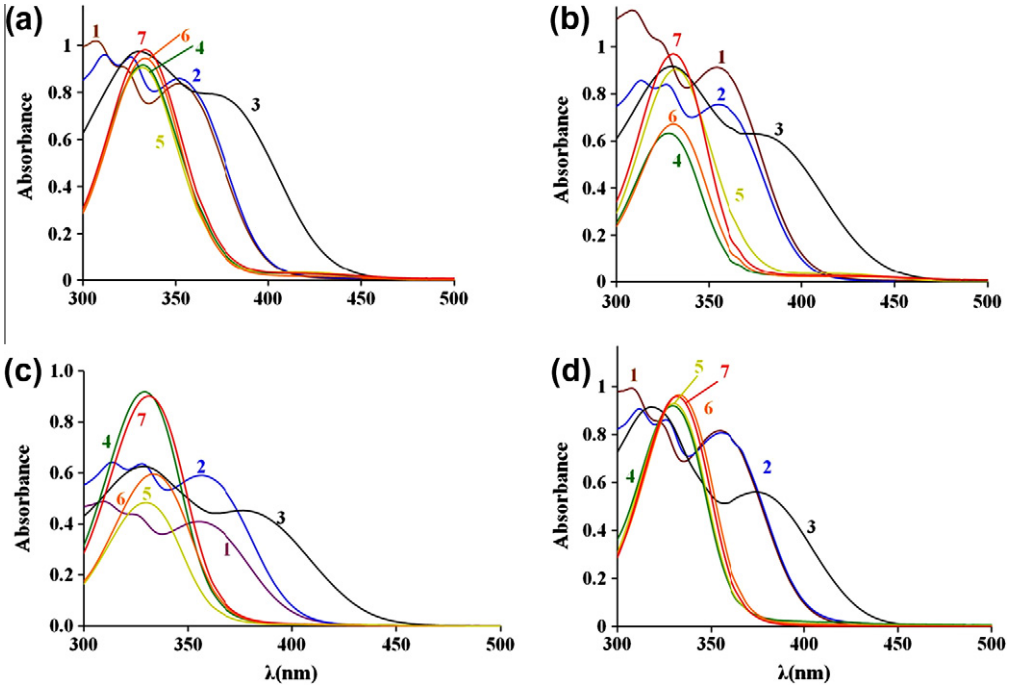

Fig. 2. UV–vis absorption spectra for **1–7** in different solvents (a) EtOH, (b) $CHCl_3$, (c) toluene, (d) n-hexane.

Table 3
The maximum absorption wavelength and absorbance for **1–7** in different solvents.

Ligands	Solvent	Wavelength λmax/[(nm) Abs(AU)]				
1	EtOH	307(1.02)	352(0.84)			
	$CHCl_3$	308 (1.16)	354(0.91)			
	Toluene	309(0.49)	354(0.41)			
	n-C_6H_{14}	307(0.99)	355(0.82)			
2	EtOH	311(0.96)	326(0.95)	352(0.86)		
	$CHCl_3$	313 (0.86)	327(0.84)	355(0.76)		
	Toluene	314(0.64)	328(0.64)	357(0.59)		
	n-C_6H_{14}	311(0.91)	326(0.86)	355(0.81)		
3	EtOH	330(0.97)				
	$CHCl_3$	330 (0.92)				
	Toluene	328(0.63)		377(0.45)		
	n-C_6H_{14}	318(0.91)		374(0.56)		485(0.004)
4	EtOH	332(0.92)				
	$CHCl_3$	328 (0.63)				488(0.008)
	Toluene	329(0.92)				
	n-C_6H_{14}	329(0.92)				492(0.007)
5	EtOH	332 (0.91)			412(0.04)	
	$CHCl_3$	328 (0.64)			421(0.02)	
	Toluene	330(0.48)				
	n-C_6H_{14}	330(0.93)				
6	EtOH	333(0.95)				
	$CHCl_3$	330 (0.67)				488(0.008)
	Toluene	332(0.60)				
	n-C_6H_{14}	333(0.97)				488(0.002)
7	EtOH	333(0.98)				
	$CHCl_3$	330 (0.97)				
	Toluene	331(0.90)				
	n-C_6H_{14}	333(0.97)				488(0.002)

conjugation should cause bathochromic shifts in the absorption maxima of chromophores and the observed bathochromic shifts with **1–3** are attributed to the partial conjugation between CH=N and the neighboring phenyl group. Absorption spectra of **1–3** exhibit 2 or 3 intense bands between 307 and 377 nm. In addition, the presence of electron releasing or withdrawing group at the *p*-position of the phenyl ring affects the absorption maxima of chromophores. The electronic spectrum of **1** with *p*-H, in both polar and nonpolar solvents shows two bands at around 308 and 353 nm, while three intense bands at around 312, 326 and

355 nm are observed for **2**, which has an electron releasing methyl group at the *p*-position. Compound **3,** with an electron withdrawing *p*-nitro group, gives two bands at around 328 and 374 nm.

In a more detailed analysis of the spectra of **3**, **4**, **6** and **7** a very weak absorption above 480 nm is detectable in nonpolar solvents. In the case of **5**, a similar, very weak absorption band that appears at 412 nm in protic polar solvent is red shifted to 421 nm in $CHCl_3$. These absorptions may be due to the presence of traces of the keto form. It was earlier considered that a bulky *o*-substituent on a phenoxy moiety, simply for steric reasons, could compel the O**H** proton to be close to the N atom and thus favor the keto tautomer [53(a)]. To confirm the effect of a *tert*-butyl group in keto-enol tautomerization, a new series of salicylaldimines without the *tert*-butyl groups (**1'**–**7'**) were also synthesized and examined in various solvents (see Supplementary materials). Of those, only salicylaldimines with *N*-phenyl (**1′**) and *N*-*p*-methylphenyl (**2′**) imine substituents show a weak absorption band at longer wavelengths than 480 nm in nonpolar solvents. In addition, *N*-*p*-nitrophenyl substituted **3′** exhibits a weak absorption band both in polar and nonpolar solvents.

To summarize, the presence of substantial absorption bands for **1**–**7** within the region of λ_{max} = 307–377 nm and the IR and NMR studies above reveal that the enol form is the predominant species in solution. Very weak absorption at 400–500 nm indicates that only minor amounts of keto tautomer are present. The influence, if there is any, of *tert*-butyl groups on keto-enol tautomerization within the series is minor and cannot be unambiguously detected [53,43].

In general, the absorption spectra of salicylaldimines in polar hydrogen bonding solvents such as MeOH and EtOH give a solvatochromic band around 400 nm. This arises from intermolecular hydrogen bonding between guest and host molecule [54–56]. It has also been reported that in aprotic polar solvent the solvatochromic band appears around 400–480 nm for salicylaldimines that have a spacer between the imine N and the phenyl ring [57,58]. The spacer eliminates the resonance of the N lone pair with the π system of phenyl; thus the basicity of the N atom increases [59]. Surprisingly, solvatochromism does not appear in the *tert*-butyl substituted **1**–**7** but a strong solvatochromic band is observed at around 400 nm for **4′**–**7′**, which have *N*-alkyl and *N*-alkylphenyl groups, respectively (see Supplementary materials, Fig. S1). This agrees with previous reports for **6′** (*N*-(benzyl) salicylaldimine) and **7′** (*N*-(2-phenylethyl) salicylaldimine) [57(a),60]. It seems that the steric bulkiness of the *tert*-butyl groups in **1**–**7** on the proximity of O–H···N hampers the formation of an intermolecular hydrogen bond between the imine and a solvent molecule [33,54–56].

3.3. Crystal structures of *1*–*7*

Compounds **1**–**7** were crystallized and their solid state structures are shown below. They all have the enol-imino conformation with an (E)-configured imine. As a consequence of a strong intramolecular hydrogen bond (O1–H1···N8), the salicylaldimine moieties form nearly planar six-membered rings [61]. The phenol ring is only slightly rotated relative to the imine moiety (between 0.8° and 9.8°), while the aromatic substituents in **1**, **2** and **3** are twisted by 24° (**1**), 31°/37° (**2**) and 39° (**3**) relative to the salicylaldimine plane. Selected bond distances and angles are given as Supplementary material and hydrogen bond geometries are listed in Table 4. Only for **1**, **4** and **5** weak cooperative intermolecular C–H···O(phenol) hydrogen bonds are found, while in **3** the NO_2-group is involved in weak intermolecular hydrogen bonds (see Table 4) [62]. The crystal structures of **1**–**7** including atom numbering schemes are shown in Figs. 3–9.

Crystallographic analysis reveals that the bond distances in the phenolic ring of salicylaldimines **1**–**7** follow the blinking sequence: C1–C2 > C2–C3 < C3–C4 > C4–C5 < C5–C6 > C6–C1, which is a typical resonance form in enol tautomers. The differences between the shortest and longest bond distances are about 0.03 Å. In the case of the keto form, the distances vary between 0.06 and 0.08 Å [47(a),48]. In general, the average C1–O1 (1.360(4) Å), C6–C7 (1.462(6) Å) and C7 = N8 (1.286(5) Å) bond distances are in good accordance with literature values (C_{ar}–OH 1.362(15) Å, C_{ar}–C_{sp2}

Table 4
Hydrogen bond geometry (Å, °).

Ligands	D–H···A	*d*(D–H)	*d*(H···A)	*d*(D···A)	∠(DHA)	σ_H[c]/Δ_H[d]
Intramolecular hydrogen bond						
1	O1–H1···N8	0.883(14)	1.748(15)	2.5656(15)	152.8(17)	0.011/0.04
2[a]	O1–H1···N8	0.848(18)	1.81(2)	2.585(3)	152(3)	0.024/0.05
		0.868(17)	1.76(2)	2.563(3)	154(3)	0.004/0.00
3	O1–H1···N8	0.877(15)	1.831(16)	2.6467(19)	153.8(19)	0.006/0.02
4[b]	O1–H1···N8	0.862(12)	1.774(16)	2.572(2)	153.0(19)	0.004/0.06
		0.864(13)	1.774(16)	2.579(2)	154.0(19)	0.001/0.05
		0.868(13)	1.732(15)	2.550(2)	156.0(19)	0.010/0.00
5	O1–H1···N8	0.864(19)	1.83(3)	2.620(5)	151(5)	0.06/0.17
6	O1–H1···N8	0.871(19)	1.76(2)	2.579(3)	156(4)	0.013/0.02
7	O1–H1···N8	0.858(16)	1.804(18)	2.604(2)	154(2)	0.006/0.04
Weak intermolecular hydrogen bonds[e]						Symmetry code
1	C11–H1···O1	0.95	2.65	3.561(2)	161.3	0.5 + *x*, 1.5 − *y*, *z*
2[a]	None					
3	C42–H42c···O16	0.98	2.67	3.609(3)	160.2	1.5 − *x*, *y*, −0.5 + *z*
	C5–H5···O17	0.95	2.59	3.492(2)	157.8	−0.5 + *x*, 1 − *y*, 1.5 − *z*
4[b]	C7–H7···O1b	0.95	2.54	3.242(3)	130.7	
	C7a–H7a···O1	0.95	2.60	3.272(3)	128.2	
	C7b–H7b···O1a	0.95	2.56	3.272(3)	132.3	1 − *x*, 1 − *y*, 1 − *z*
5	C44–H44b···O1	0.98	2.63	3.538(5)	153.5	1.5 − *x*, −0.5 + *y*, 0.5 + *z*
6	None					
7	None					

[a] Two independent molecules in the asymmetric unit.
[b] Three independent molecules in the asymmetric unit.
[c] Mean deviation from the plane O1–C1–C6–C7–N8.
[d] Deviation of H1 from the plane O1–C1–C6–C7–N8.
[e] Refs. [61,62].

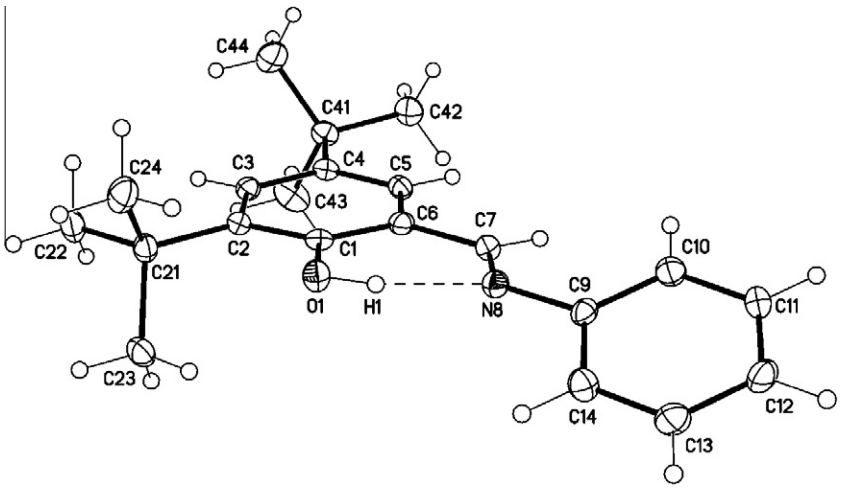

Fig. 3. Molecular structure of **1** (displacement parameters are drawn at 50% of the probability level).

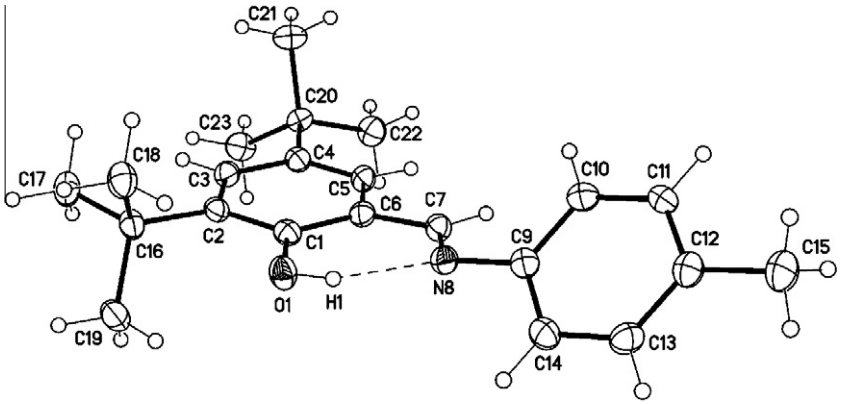

Fig. 4. Molecular structure of **2**, one of the two independent molecules (displacement parameters are drawn at 50% of the probability level).

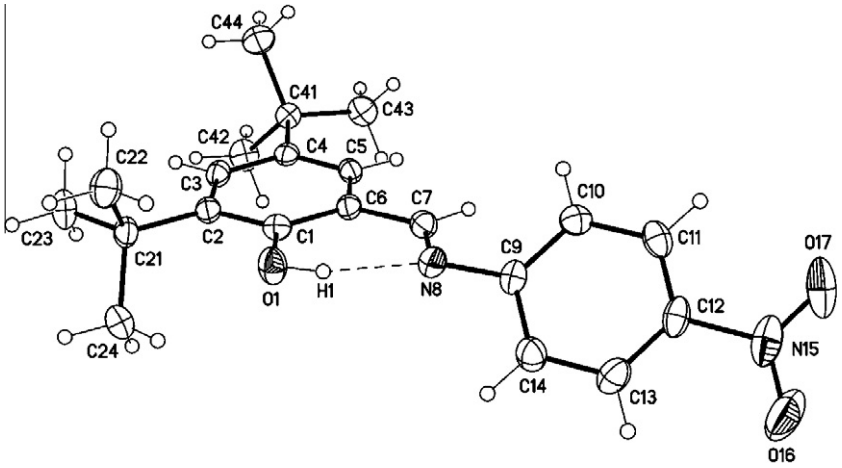

Fig. 5. Molecular structure of **3** (displacement parameters are drawn at 50% of the probability level).

(conjugated) 1.470(15) Å, C_{ar}–C_{sp2} (unconjugated) 1.488(12) Å, C_{sp2}=$N_{(2)}$ 1.279(8) Å) [63,64]. The C=N bond distances of *N*-alkyl (**4**–**5**), *N*-alkyl phenyl (**6**–**7**) and *N*-phenyl (**1**–**3**) salicylaldimines are 1.277–1.283 Å, 1.282–1.286 Å and 1.287–1.298 Å, respectively. A slight lengthening of the C=N bond in *N*-phenyl salicylaldimines is explained by the electron withdrawing phenyl group. The distances (N8–C9) between imine N atoms and C atoms of phenyl or alkyl groups are 1.422(2) –1.477(3) Å, corresponding to the C–N

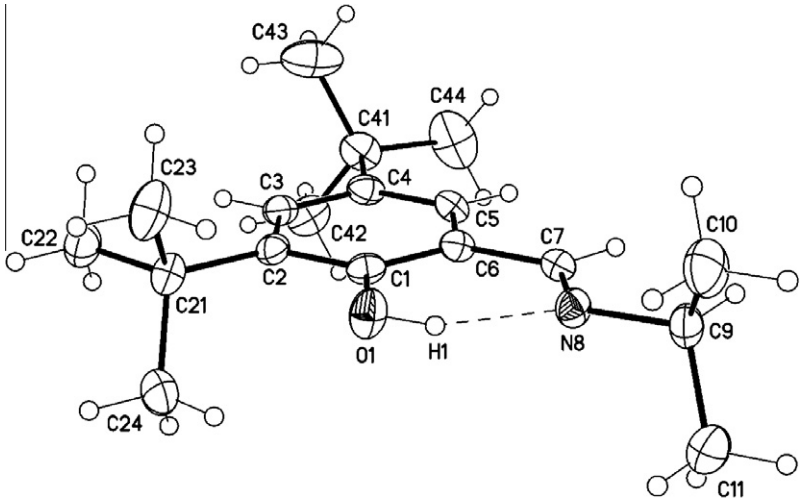

Fig. 6. Molecular structure of **4**, one of the three independent molecules (displacement parameters are drawn at 50% of the probability level).

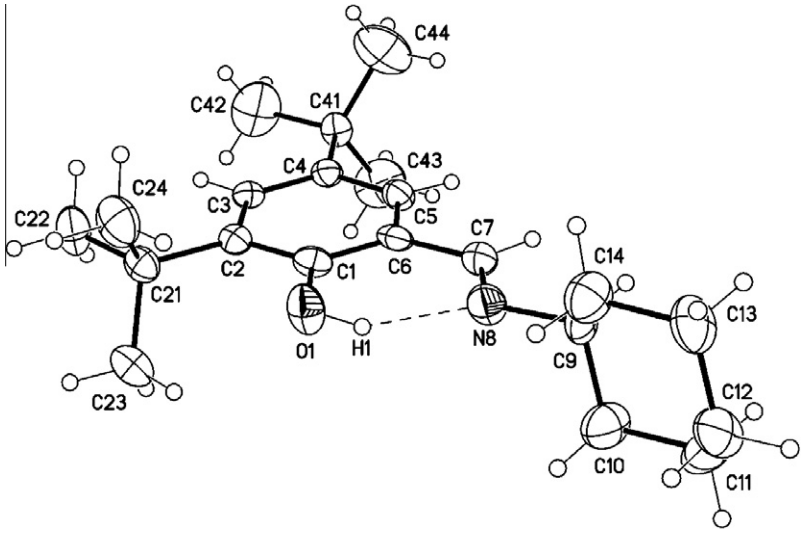

Fig. 7. Molecular structure of **5** (displacement parameters are drawn at 50% of the probability level).

single bond (1.469 Å) [63,64]. All other bond distances and angles of the phenyl rings of parent amine and *tert*-butyl groups are within expected values.

The existence of intramolecular hydrogen bonds between the phenolic hydroxyl oxygen and azomethine nitrogen in solid state has been studied for various Schiff base derivatives. According to the literature [47(a),48,64–67], the O···N distance is significantly shorter (for example, 2.555 Å in *N*-(*p*-nitrophenyl) salicylaldimine, 2.604(3) Å in *N*-(2-methyl-5-chlorophenyl) salicylaldimine, 2.598(2) Å in *N*-(3-methoxyphenyl) salicylaldimine, 2.515(2) in *N*-(2-hydroxy-5-chlorophenyl) salicylaldimine) than the sum of their Van der Waals radii (3.07 Å). In **1**–**7**, the O···N distance ranges from 2.550 to 2.647 Å due to the presence of strong intramolecular hydrogen bonding.

The most significant indicator of the type of tautomeric form is the bond distances within the six-membered ring. The C–O bond distances in the enol form are a bit longer than those observed in the keto form due to the double bond character of the latter. The distinctive C–O bond distances of *N*-phenyl (**1**–**3**), *N*-alkyl phenyl (**6**–**7**) and *N*-alkyl (**4**–**5**) salicylaldimines are 1.352–1.359 Å, 1.358–1.362 Å and 1.362–1.365 Å, respectively. These are apparently values for single bonds, i.e. for the enol tautomers. Because of the double bond character of the keto form, the bond distances appear to be clearly shorter, varying from 1.268 to 1.312 Å [29,37].

The bond distances between the azomethine N and hydroxyl H are also longer in the enol form than in the keto form. The H···N distances for **1**–**7** are in the range of 1.76–1.83 Å, being substantially longer than those reported for the keto (N–H) form, 1.03–1.11 Å [68]. It can be concluded that **1**–**7**, irrespectively of any electron releasing (Me) or withdrawing (NO_2) group, have the enol tautomeric form. This is accordance with their solution structures.

3.4. Computational results

To study the relative stability of the two possible tautomers, their respective geometries were fully optimized. No internal coordinates have been frozen. The experimental atomic coordinates from the X-ray studies were used as input for the enol form. Then the optimized structure was modified to the corresponding keto tautomer, and the structure was reoptimized (see Supplementary materials). In each keto-enol pair the enol form is more stable,

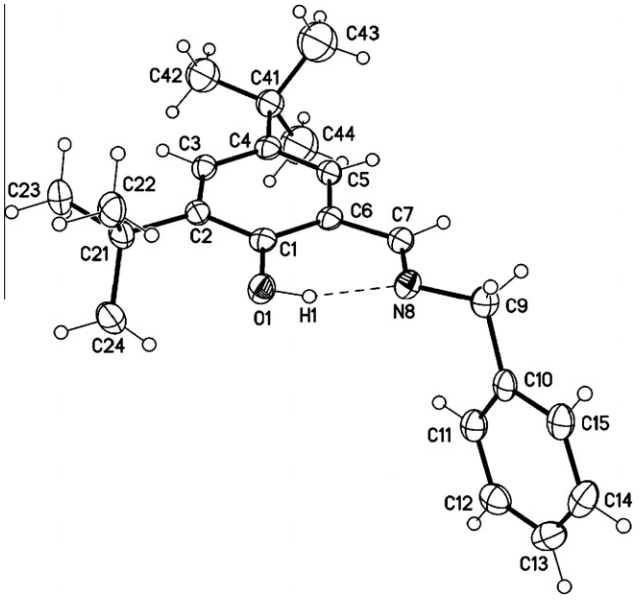

Fig. 8. Molecular structure of **6**, minor disordered component omitted for clarity (displacement parameters are drawn at 50% of the probability level).

although the differences in energy vary from 5.5 to 10.1 kJ/mol (in terms of total energy obtained from Gaussian for the optimized moieties). It must be noted that in the solid state there are intermolecular hydrogen bonds that might stabilize one of the tautomers more than the other.

As shown in the crystallographic study, all of the studied salicylaldimines belong to the point group C_1 in the solid state. However, as stated in Ref. [12], there also exists the possibility that the molecules can display a higher symmetry. Accordingly, two sets of salicylaldimines were optimized. In the first set the experimental atomic coordinates were used as input, whereas for the second set the molecules were optimized in the point group C_s. In the latter set only the optimized molecules with an aliphatic substituent (**4**–**5**) represented the real energy minimum in their potential energy surfaces. The optimized salicylaldimines represented the lowest energy for each compound (see Supplementary materials). Selected geometrical parameters are given in Tables 5 and 6.

Variation in the geometrical parameters for the optimized compounds is small. Notable variation is seen only in the N8–C9 bond distance, which is formally a single bond. The longest values for the N8–C9 bonds are found in the cases where the carbon atom is aliphatic. The Wiberg bond indices show clearly, that there are no pure single or double bonds connecting the atoms C1, C6, C7 and N8. Instead, the values are suggestive of electron delocalization. To further characterize the bonding in the molecules, NBO analysis was also carried out. Calculated natural charges are shown in Table 7.

There is a clear trend in the six-membered ring stabilized by hydrogen bonding: starting from H1 to N8 the charges are alternately positive and negative. Interestingly, the charge at C9 clearly varies. When carbon C9 is aromatic, it always carries a positive charge. When the carbon is aliphatic, the charge is negative.

In order to get an insight into the equilibrium between the keto and enol forms, second order perturbation analysis of Fock matrix in NBO basis was carried out. The results are shown in Table 8. In the enol form there is a stabilizing charge transfer from the electron lone pair of nitrogen into the O–H antibonding molecular orbi-

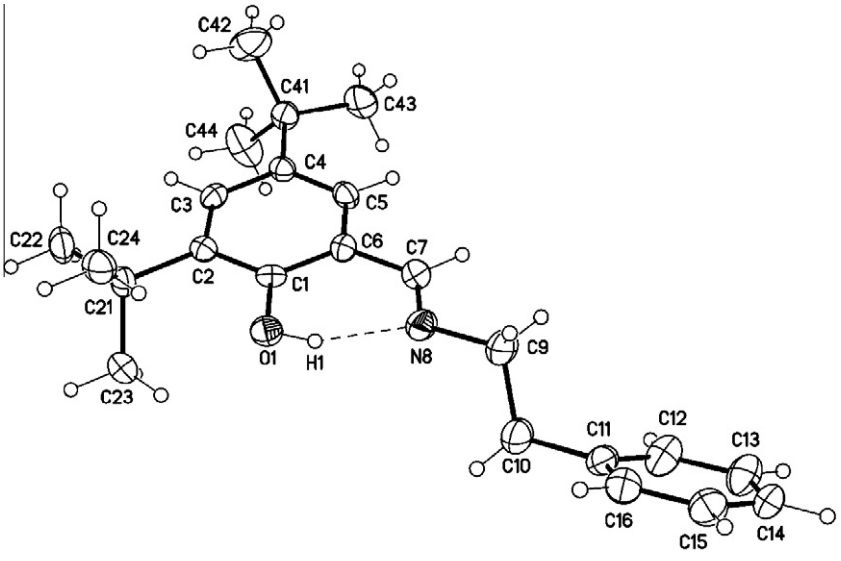

Fig. 9. Molecular structure of **7** (displacement parameters are drawn at 50% of the probability level).

Table 5
Selected bond distances (Å) and bond angles (°) for the optimized compounds showing energy minima at the B3LYP/6–311G* level of theory.

Compound	Point group	C7=N8	N8···H1	N8···O1	O1–H1	N8–C9	O1–C1–C6	C1–C6–C7	C6–C7–N8	C7–N8–C9
1	C_1	1.289	1.727	2.621	0.993	1.408	120.37	121.61	123.22	121.41
2	C_1	1.288	1.733	2.627	0.992	1.408	120.18	121.77	123.27	121.30
3	C_1	1.292	1.741	2.630	0.990	1.400	120.44	121.74	123.45	121.29
4	C_s	1.280	1.727	2.624	0.993	1.460	120.30	121.36	123.63	119.86
5	C_s	1.285	1.723	2.631	1.001	1.457	120.00	121.58	123.56	119.88
6	C_1	1.280	1.728	2.623	0.993	1.449	120.16	121.46	123.46	119.54
7	C_1	1.281	1.725	2.622	0.993	1.451	120.29	121.36	123.60	119.66

Table 6
Selected dihedral angles (°) for the optimized compounds showing energy minima at the B3LYP/6–311G* level of theory.

Compound	Point group	O1–C1–C6–C7	C1–C6–C7–N8	C6–C7–N8–C9	H–O1–C1–C6
1	C_1	−0.09	0.46	−177.45	0.21
2	C_1	0.27	−0.64	177.35	0.15
3	C_1	−0.33	0.81	−176.82	−0.35
4	C_s	0.00	0.00	180.00	0.00
5	C_s	0.00	0.00	180.00	0.00
6	C_1	−0.02	−0.74	−179.54	2.00
7	C_1	−0.42	0.38	−179.85	−0.33

Table 7
Natural charges for the optimized compounds calculated at the B3LYP/6–311G* level of theory.

Atoms	**1**	**2**	**3**	**4**	**5**	**6**	**7**
H1	0.498	0.498	0.498	0.497	0.497	0.499	0.497
O1	−0.690	−0.692	−0.683	−0.696	−0.697	−0.697	−0.695
C1	0.397	0.392	0.402	0.392	0.388	0.389	0.392
C6	−0.177	−0.174	−0.181	−0.175	−0.172	−0.175	−0.176
C7	0.167	0.165	0.178	0.155	0.156	0.164	0.156
N8	−0.544	−0.540	−0.553	−0.547	−0.538	−0.538	−0.538
C9	0.150	0.142	0.182	−0.001	−0.007	−0.183	−0.155

Table 8
Second order perturbation theory analysis of Fock matrix. Stabilization energies in kcal/mol.[a]

Ligands	**1**	**2**	**3**	**4**	**5**	**6**	**7**
Enol $\sigma^n(N) \rightarrow \sigma^a(O–H)$	25.54	24.82	23.64	n.d.	25.18	25.17	25.82
Keto	16.65	17.84	16.79	15.56	16.65	16.61	15.47
	3.72	*3.82*	*3.74*	*3.57*	*3.72*	*3.66*	*3.47*
$\sigma^n(O) \rightarrow \sigma^a(N–H)$	20.37	21.66	20.53	19.13	20.37	20.27	18.94
Difference	5.17	3.16	3.11	–	4.81	4.90	6.88

n.d., not detected.
[a] In the keto form the minor component is shown italics and the sum value is underlined.

tal. In the keto form the corresponding charge transfer occurs between two lone pairs of oxygen into the N–H antibonding molecular orbital. The two contributions in terms of stabilizing energy are not equal. However, the sum of the energies is always smaller for the keto forms than the value in the corresponding enol form. The smallest difference is found for the compounds **2** and **3**. Both of these have a *p*-substituted phenyl ring connected to nitrogen.

4. Conclusions

A series of sterically hindered, 3,5-di-*tert*-butyl salicylaldimine derivatives were synthesized and characterized by spectroscopic methods. Solid state structures of the compounds were determined by X-ray crystallography. In solid state, regardless of whether there was an electron releasing (Me) or withdrawing (NO_2) group, all molecules possessed a strong intramolecular hydrogen bond (O1–H···N8), forming a nearly planar six-membered ring. According to UV–vis, IR and NMR studies, this structure is also present in solution. Computational results also revealed that in each keto-enol pair, the enol form is more stable and the differences in energy vary from 5.5 to 10.1 kJ/mol. It is noteworthy that the *tert*-butyl groups in **1**–**7**, due to their bulkiness and proximity to the O–H···N hydrogen bond, hamper the formation of an intermolecular hydrogen bond between the imine and a solvent molecule. Due to the strong intramolecular hydrogen bonding between the phenol group and the imine nitrogen the structures of the ligands are already preorganized and act as a bidentate chelate ligand rather than a bridging ligand in complexation reactions.

Acknowledgments

Financial support from the Graduate School of Inorganic Material Chemistry and the International Student Grant of University of Helsinki is gratefully acknowledged. MRS acknowledges the generous computing time given by CSC (CSC–IT Center for Science Ltd., Finland).

Appendix A. Supplementary material

Supplementary data associated with this article can be found, in the online version, at doi:10.1016/j.molstruc.2011.02.033.

References

[1] Q. Han, F. Jian, L. Lu, X. Yang, X. Wang, J. Chem. Crystallogr. 31 (2001) 247.
[2] A.L. Iglesias, G. Aguirre, R. Somanasamy, M.P. Hake, Polyhedron 23 (2004) 3051.
[3] H. Nozaki, H. Takaya, S. Moriuti, R. Noyori, Tetrahedron 24 (1968) 3655.
[4] Z. Zheng, M. Han, H.L. Chen, Chin. Chem. Lett. 7 (1996) 739.
[5] Z. Li, Z. Zheng, H. Cheng, Tetrahedron: Asymmetry 11 (2000) 1157.
[6] T. Aratani, Pure Appl. Chem. 57 (1985) 1839.
[7] Z. Li, M. Fernandez, E.N. Jacobsen, Org. Lett. 1 (1999) 1611.
[8] R.M. Wang, C.J. Hao, Y.P. Wang, S.B. Li, J. Mol. Catal. 147 (1999) 173.
[9] R.M. Wang, C.J. Hao, Y.F. He, Y.P. Wang, C.G. Xia, Polym. Adv. Technol. 13 (2002) 6.
[10] N. Kitajima, K. Whang, Y. Morooka, A. Uchida, Y. Sasada, J. Chem. Soc., Chem. Commun. 20 (1986) 1504.
[11] Y. Wang, T.D.P. Stack, J. Am. Chem. Soc. 118 (1996) 13097.
[12] J. Huang, B. Lian, Y. Qian, W. Zhou, W. Chen, G. Zheng, Macromolecules 35 (2002) 4871.
[13] M. Mitani, J. Mohri, Y. Yoshida, J. Saito, S. Ishii, K. Tsuru, S. Matsugi, N. Kashiwa, T. Fujita, J. Am. Chem. Soc. 24 (2002) 3327.
[14] (a) V.G. Gibson, S.K. Spitzmesser, Chem. Rev. 103 (2003) 283;
(b) T. Repo, M. Klinga, P. Pietikäinen, M. Leskelä, Macromolecules 30 (1997) 171.
[15] A. Pärssinen, T. Luhtanen, M. Klinga, T. Pakkanen, M. Leskelä, T. Repo, Organometallics 26 (2007) 3690.
[16] A. Pärssinen, T. Luhtanen, M. Klinga, T. Pakkanen, M. Leskelä, T. Repo, Eur. J. Inorg. Chem. 11 (2005) 2100.
[17] R.I. Kureshy, N.H. Khan, S.H.R. Abdi, S.T. Patel, R.V. Jasra, Tetrahedron: Asymmetry 12 (2001) 433.
[18] A. Berkessel, M. Frauenkron, T. Schwenkreis, A. Steinmetz, J. Mol. Catal. 117 (1997) 339.
[19] L. Canali, D.C. Sherrington, H. Deleuze, React. Funct. Polym. 40 (1999) 155.
[20] A.G. Dossetter, T.F. Jamison, E.N. Jacobsen, Angew. Chem., Int. Ed. Eng. 38 (1999) 2398.
[21] Z. Chenghe, G. Linling, Z. Yiyi, Z. Feifei, W. Guangzhou, J. Lei, G. Rongxi, Sci. China Ser. B – Chem. 52 (2009) 415.
[22] N.H. Gokhale, K. Shirisha, S.B. Padhye, S.L. Croft, H.D. Kendrick, V. Mckee, Bioorg. Med. Chem. Lett. 16 (2006) 430.
[23] A. Filarowski, J. Phys. Org. Chem. 18 (2005) 686.
[24] E. Hadjoudis, M. Vitterakis, I. Mavridis, Tetrahedron 43 (1987) 1345.
[25] T. Fujiwara, J. Harada, K. Ogawa, J. Phys. Chem. B 108 (2004) 4035.
[26] J. Harada, H. Uekusa, Y. Ohashi, J. Am. Chem. Soc. 121 (1999) 5809.
[27] I.M. Mavridis, E. Hadjoudis, A. Mavridis, Acta Crystallogr. B34 (1978) 3709.
[28] A. Elmali, Y. Eleman, C.T. Zeyrek, J. Mol. Struct. 443 (1998) 123.
[29] (a) M.T. Räisänen, P. Elo, M. Kettunen, M. Klinga, M. Leskelä, T. Repo, Synth. Comun. 37 (2009) 1;
(b) Z. Popovic, G. Popovic, D.M. Calogovic, V. Roje, I. Leban, J. Mol. Struct. 615 (2002) 23.
[30] J.U. Ahmad, P.J. Figiel, M.T. Räisänen, M. Leskelä, T. Repo, Appl. Catal. A 371 (2009) 17.
[31] V.T. Kasumov, A. Bulut, F. Köksal, M. Aslanoglu, I. Ucar, C. Kazak, Polyhedron 25 (2006) 1133.
[32] (a) M.J. Heravi, A.A. Khandar, I. Sheishoaie, Spectrochim. Acta A 55 (1999) 2537;
(b) K. Ogawa, Y. Kasahara, Y. Ohtani, J. Harada, J. Am. Chem. Soc. 120 (1998) 7107.
[33] K. Ogawa, J. Harada, T. Fujiwara, S. Yoshida, J. Phys. Chem. A 105 (2001) 3425.
[34] G.M. Sheldrick, Acta Crystallogr. A 64 (2008) 112.
[35] H.D. Flack, Acta Crystallogr. A 39 (1983) 876.
[36] A. Karakas, A. Elmali, H. Unver, I. Svoboda, J. Mol. Struct. 702 (2004) 103.
[37] S.D. Chatziefthimiou, Y.G. Lazarou, E. Hadjoudis, T. Dziembowska, I.M. Mavridis, J. Phys. Chem. B 110 (2006) 23701.

[38] Gaussian 03, Revision D.02, M.J. Frisch, G.W. Trucks, H.B. Schlegel, G.E. Scuseria, M.A. Robb, J.R. Cheeseman, J.A. Montgomery, Jr., T. Vreven, K.N. Kudin, J.C. Burant, J.M. Millam, S.S. Iyengar, J. Tomasi, V. Barone, B. Mennucci, M. Cossi, G. Scalmani, N. Rega, G.A. Petersson, H. Nakatsuji, M. Hada, M. Ehara, K. Toyota, R. Fukuda, J. Hasegawa, M. Ishida, T. Nakajima, Y. Honda, O. Kitao, H. Nakai, M. Klene, X. Li, J.E. Knox, H.P. Hratchian, J.B. Cross, V. Bakken, C. Adamo, J. Jaramillo, R. Gomperts, R.E. Stratmann, O. Yazyev, A.J. Austin, R. Cammi, C. Pomelli, J.W. Ochterski, P.Y. Ayala, K. Morokuma, G.A. Voth, P. Salvador, J.J. Dannenberg, V.G. Zakrzewski, S. Dapprich, A.D. Daniels, M.C. Strain, O. Farkas, D.K. Malick, A.D. Rabuck, K. Raghavachari, J.B. Foresman, J.V. Ortiz, Q. Cui, A.G. Baboul, S. Clifford, J. Cioslowski, B.B. Stefanov, G. Liu, A. Liashenko, P. Piskorz, I. Komaromi, R.L. Martin, D.J. Fox, T. Keith, M.A. Al-Laham, C.Y. Peng, A. Nanayakkara, M. Challacombe, P.M.W. Gill, B. Johnson, W. Chen, M.W. Wong, C. Gonzalez, J.A. Pople, Gaussian, Inc., Wallingford, CT, 2004.
[39] F. Weinhold, F.C. Landis, Valency and Bonding – A Natural and Orbital Donor–Acceptor Perspective, Cambridge University Press, Cambridge, 2005.
[40] (a) I. Sheikhshoaie, V. Saheb, Spectrochim. Acta Part A 77 (2010) 1069;
(b) M. Karabacak, M. Cinar, M. Kurt, J. Mol. Stuct. 885 (2008) 28.
[41] J.L. van Wyk, S.F. Mapolie, A. Lennartson, M. Hakansson, S. Jagner, Inorg. Chim. Acta 361 (2008) 2094.
[42] C. Topacli, A. Topacli, J. Mol. Struct. 654 (2003) 131.
[43] V.T. Kasumov, F. Köksal, A. Sezer, Polyhedron 24 (2005) 1203.
[44] V.T. Kasumov, F. Köksal, R. Koseoglu, J. Coord. Chem. 57 (2004) 591.
[45] G.C. Perey, D.A. Thmton, J. Inorg. Nucl. Chem. 34 (1972) 3357.
[46] G.J.M. Femandez, F. Del Rio-Portila, B. Quiroz-Garcia, R.A. Toscano, R. Salcedo, J. Mol. Struct. 561 (2001) 197.
[47] (a) H. Pizzala, M. Carles, W.E.E. Stone, A. Thevand, J. Chem. Soc., Perkin Trans. 2 (2000) 935;
(b) A.L. Iglesias, G. Aguirre, R. Somanathan, M. Parra-Hake, Polyhedron 23 (2004) 3051.
[48] S.H. Alarcon, A.C. Olivieri, R.M. Cravero, G. Labadie, M. Gonzalez-Sierra, J. Phys. Org. Chem. 8 (1995) 713.
[49] M. Ottolenghi, S.D. McClure, J. Chem. Phys. 46 (1967) 4613.
[50] S.L. Mulov, Handbook of Photochemistry, Mercel Dekker, New York, 1973. p. 86.
[51] (a) G.O. Dudek, E.P. Dudek, J. Am. Chem. Soc. 88 (1966) 2407;
(b) E. Tas, V.T. Kasumov, O. Sahin, M. Ozdemir, Trans. Metal Chem. 27 (2002) 442.
[52] P. Nagy, R. Herzfeld, Spectrosc. Lett. 31 (1998) 221.
[53] (a) S.R. Salman, S.H. Shawkat, F.S. Kamounah, Can. J. Appl. Spectrosc. 37 (1992) 46;
(b) S.R. Salman, N.A.I. Saleh, Spectrosc. Lett. 30 (1997) 1289.
[54] A. Grabowska, K. Kownacki, J. Karpiuk, S. Dobrin, L. Kaczmarek, Chem. Phys. Lett. 267 (1997) 132.
[55] T. Sekikawa, T. Kobayashi, T. Inabe, J. Phys. Chem. A 101 (1997) 644.
[56] A. Mandal, D. Fitzmaurice, E. Waghorne, A. Koll, A. Filarowski, D. Guha, S. Mukherjee, J. Photochem. Photobiol., A 153 (2002) 67.
[57] S.R. Salman, S.H. Shawkat, G.H. Al-Obaidi, Can. J. Spectrosc. 35 (1990) 25.
[58] S.R. Salman, S.H. Shawkat, G.H. Al-Obaidi, Spectrosc. Lett. 22 (1989) 1156.
[59] E. Lambi, D. Gegiou, E. Hadjoudis, J. Photochem. A: Chem. 86 (1995) 241.
[60] (a) D. Gegiou, E. Lambi, E. Hadjoudis, J. Phys. Chem. 86 (1995) 241;
(b) S.R. Salman, S.K. Kanber, L.K. Arsalan, Spectrosc. Lett. 24 (1991) 1153.
[61] T. Steiner, Angew. Chem. Int. Ed. 41 (2002) 48.
[62] G.R. Desiraju, T. Steiner, The Weak Hydrogen Bond in Structural Chemistry and Biology, Oxford University Press, Oxford, 1999.
[63] A.J.C. Wilson (Ed.), International Table for Crystallography, Vol. C, Kluwer Academic, Dordrecht, 1992, p. 685 (Chapter 9.5).
[64] A.G. Orpen, L. Brammer, F.H. Allen, O. Kennard, D.G. Watson, R. Taylor, in: H.-B. Burgi, J.D. Dunitz (Eds.), Structure Correlation, vol. 2, VCH, Weinheim, 1994, p. 751.
[65] A. Elmali, Y. Eleman, J. Mol. Struct. 442 (1998) 31.
[66] A. Elmali, M. Kabak, Y. Eleman, J. Mol. Struct. 484 (1999) 229.
[67] A. Elmali, M. Kabak, E. Kavlakoglu, Y. Eleman, T.N. Durlu, J. Mol. Struct. 510 (1999) 207.
[68] A. Filarowski, A. Koll, T. Glowiak, J. Chem. Soc. Perkin Trans. 2 (2002) 835.